

Supporting Information

1. PXRD, EDS and IR spectrum of NNU-5

The powder XRD pattern of NNU-5 is in agreement with the simulated XRD pattern based on single-crystal structural data, proving the phase purity of the as-synthesized product as given in Fig. S5. The chemical composition of NNU-5 was confirmed by the results of EDS, which indicated the presence of the elements Cd, V, B and O (Fig. S6). From the IR spectrum of NNU-5 (KBr pellet), the observed bands at 3433 and 1632 cm^{-1} can be attributed to the stretching and bending vibrations of -OH groups and H_2O molecules, which clearly indicates the presence of -OH groups and water molecules in the crystal structure of NNU-5. Bands at 1456 and 1394 cm^{-1} correspond to the stretching and bending vibrations of BO_3 groups, while the bands in the region of 1055–541 cm^{-1} (1055, 941, 831, 795, 721, 669 and 541 cm^{-1}) can be assigned to the asymmetric stretching and bending vibrations of VO_5 , BO_4 and V–O–B groups.

2. Thermal stability of NNU-5

The thermal stability was investigated between room temperature and 800 °C with a heating rate of 10 °C \cdot min⁻¹ in a dynamic N_2 atmosphere (gas flow 0.1 L \cdot min⁻¹). The studies reveal a total mass loss of 14.74 % between 75 and 800 °C in three steps ($\Delta m_{\text{calcd}}/m = 14.32\%$). In the DTG curve, four significant peaks were observed, at 325 °C, 370 °C, 518 and 577 °C. In the first step, between 75 and 360 °C, the weight is reduced by 7.93 %, which agrees well with the release of 10 molecules of water per formula unit ($\Delta m_{\text{calcd}}/m = 7.51\%$) and with the first peak observed in the DTG measurement ($T = 325$ °C). It is interesting to note that the first process is reversible. The dehydrated sample in the first step shows nearly the same mass loss again when exposed to air for three days. In the second step of mass loss, between 360 and 407 °C, the weight is reduced by 4.04%, which reveals the loss of 3 molecule of coordinated water ($\Delta m_{\text{calcd}}/m = 4.50\%$) and with the second peak observed in the DTG measurement ($T = 370$ °C). In the last step, between 407 and 629 °C, the weight decreases by another 2.77 %, which matches the loss of 3 molecule of water (6 -OH groups, $\Delta m_{\text{calcd}}/m = 2.31\%$). The three-step behavior in TG and DTG measurements indicates that the decomposition of the 3-D cadmium borovanadate framework should be in the third step ($T = 518$ and 577 °C).

3. The discussion of the synthetic procedures

The red block crystals were picked out and washed with deionized water, purified ultrasonically, and air-dried to give a yield of *ca.* 57% (based on $\text{Cd}(\text{NO}_3)_2 \cdot 4\text{H}_2\text{O}$). All the following characterizations and properties of NNU-5 were based on the picked out crystals. It's important to note that ethylenediamine as reducing agent plays a crucial role in the formation of variable oxidation states (V^{IV} and V^{V}). The compound NNU-5 could also be obtained using $\text{Na}_2\text{B}_4\text{O}_7 \cdot 10\text{H}_2\text{O}$ as boron source instead of H_3BO_3 ($n(\text{Na}_2\text{B}_4\text{O}_7 \cdot 10\text{H}_2\text{O}) : n(\text{H}_3\text{BO}_3) = 1 : 4$). However, it was not successful in the attempts to prepare the compound NNU-5 analog using other boron source B_2O_3 instead of phenyl boric acid ($n(\text{B}_2\text{O}_3) : n(\text{phenyl boric acid}) = 1 : 2$). When the amount of ethylenediamine was increased two times ($n(\text{ethylenediamine}) : n(\text{Cd}(\text{NO}_3)_2 \cdot 4\text{H}_2\text{O}) = 15 : 1$), black block crystals of $(\text{enH}_2)_5(\text{H}_3\text{O})_2[(\text{V}^{\text{IV}}\text{O})_{12}\text{O}_6\text{B}_{18}\text{O}_{36}(\text{OH})_6] \cdot 6\text{H}_2\text{O}$ were obtained as a single-phase product with a yield of 42 % (based on $\text{Cd}(\text{NO}_3)_2 \cdot 4\text{H}_2\text{O}$).

4. The detailed absorption properties

According to the result of PLATON analysis which performed only on the framework structure $[\text{Cd}^{\text{II}}_3(\text{H}_2\text{O})_6][(\text{V}^{\text{IV}}\text{O})_6(\text{V}^{\text{V}}\text{O})_6\text{O}_6(\text{B}_{18}\text{O}_{36}(\text{OH})_6)]$ (the isolated water molecules have been removed), we found that it exists the solvent accessible voids. Therefore, we try to study the sorption property of the framework $[\text{Cd}^{\text{II}}_3(\text{H}_2\text{O})_6][(\text{V}^{\text{IV}}\text{O})_6(\text{V}^{\text{V}}\text{O})_6\text{O}_6(\text{B}_{18}\text{O}_{36}(\text{OH})_6)]$ (the isolated water molecules have been removed). Herein, we use the dehydrated samples as research subjects, the dehydrated samples came from the product after the first step of TG analysis (below 360 °C)---the sample only lost the isolated water molecules. The products were cooled down the temperature, they were added into 20 mL methanol, 20 mL alcohol and 20 mL *n*-propanol at room temperature under stirring for 24 h, respectively. Then the samples were washed repeatedly with deionized water and air-dried at room temperature. By means of IR spectra, we investigated whether the molecules could be adsorbed. Through

the analysis on the C-H characteristic peaks of IR spectra, we found that only methanol and alcohol molecules could be adsorbed and *n*-propanol molecule could not (Fig. S4). This is perhaps owing to the smaller molecular volume of methanol and alcohol than *n*-propanol.

5. Further investigations of catalytic reaction

After completion of the catalytic reaction, the catalyst can easily be separated from the reaction mixture by centrifugation and filtration. The recovered catalyst was washed repeatedly with deionized water, air-dried at room temperature and further reused in the subsequent catalytic reactions. In addition, the catalytic activities of the recovered catalyst were also investigated under the same conditions. The experimental results are listed as follows: the conversion of cyclohexanol is *av.* 54.4 %, 53.9% and 53.7%, respectively (Here, each *av.* conversion of cyclohexanol depends on the results of three parallel experiments). The results display that there is no obvious loss of catalytic activity after three runs, which shows the compound owns high recyclability.

6. Figure captions:

Figure S1. (a) Coordination environments of the Cd, V and B atoms in **NNU-5** (none-coordinated water molecules are omitted for clarity). Atoms with the additional “A–E” letters in the atom labels are at equivalent positions (A: $1.5-x, y, 0.5-z$; B: $1+y, 0.5-z, 1.5-x$; C: $1-y, -0.5+z, -0.5+x$; D: $0.5+z, 1-x, 0.5+y$; E: $1-z, -0.5+x, 0.5+y$).

Figure S2. The structure of borophosphate anion **NNU-5a**

Figure S3. The 6-connected topology of the 3-D open-framework cadmium cadmium(II) borovanadate. Colour code: borovanadate anions **NNU-5a**: blue; CdO_6 , red.

Figure S4. The IR spectra of the sorption for methanol, ethanol and *n*-propanol, respectively

Figure S5. The simulated XRD pattern and PXRD patterns of the compound **NNU-5** collected before and after the catalytic reactions.

Figure S6. The EDS for the single crystal of **NNU-5**

Table S1. Crystal data and structure refinement for **NNU-5**

Table S2. Selected bond lengths and angles for **NNU-5**

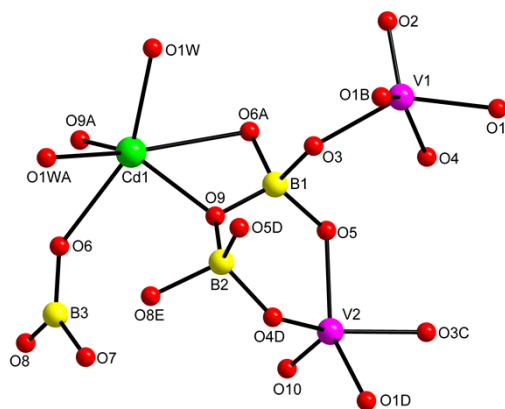


Figure S1

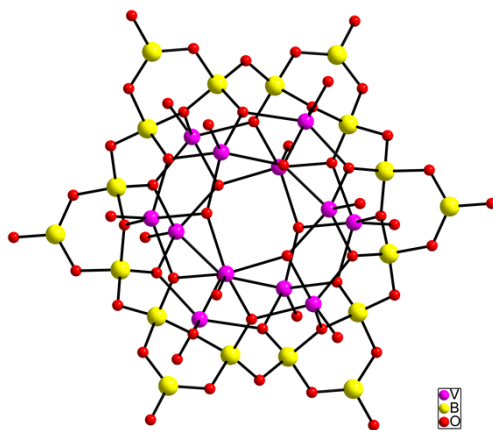


Figure S2

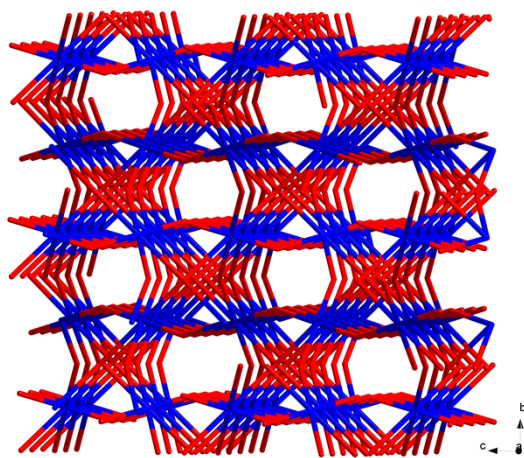


Figure S3

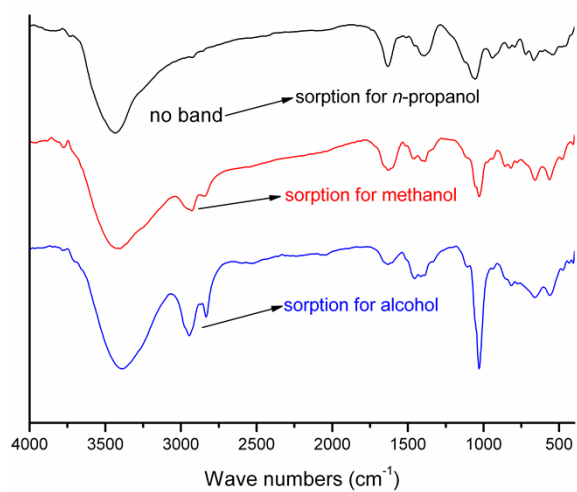


Figure S4

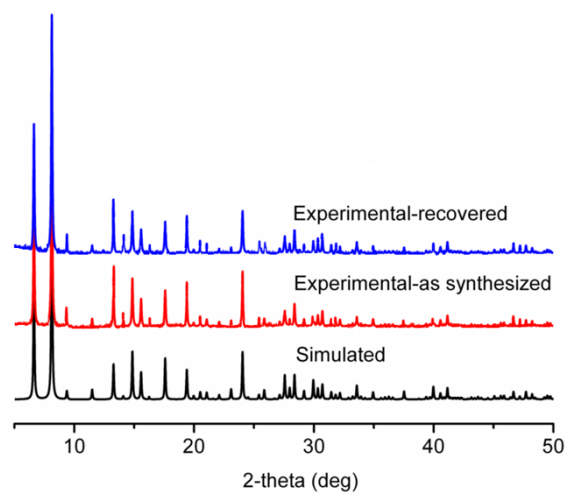


Figure S5

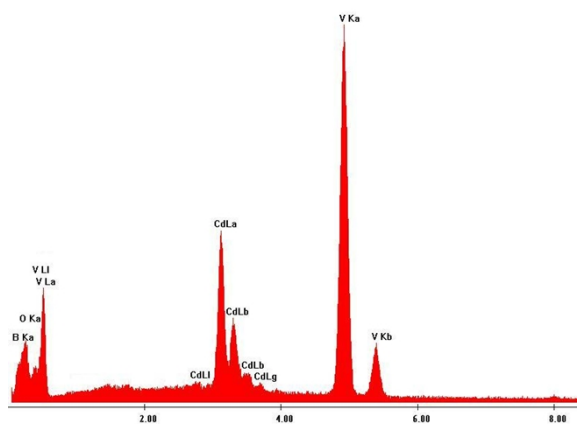


Figure S6

Table S1

Identification code	NNU-5
Empirical formula	B ₁₈ H ₃₂ Cd ₃ O ₇₆ V ₁₂
Formula weight	2397.20
Temperature/K	293(2)
Crystal system	cubic
Space group	<i>Pn</i> -3 (No. 201)
<i>a</i> /Å	18.852(9)
<i>V</i> /Å ³	6700(6)
<i>Z</i>	4
<i>D</i> _c /g·cm ⁻³	2.357
<i>μ</i> /mm ⁻¹	2.659
<i>F</i> (000)	4544
Reflections collected	31877
Unique data	1931
Goodness-of-fit on <i>F</i> ²	1.039
<i>R</i> ₁ ^a [<i>I</i> >2σ(<i>I</i>)]	<i>R</i> ₁ = 0.0936
<i>wR</i> ₂ ^b [<i>I</i> >2σ(<i>I</i>)]	<i>wR</i> ₂ = 0.1828

^a*R*₁ = Σ||*F*_o| - |*F*_c||/Σ|*F*_o|. ^b*wR*₂ = [Σ(*w*(*F*_o² - *F*_c²)²)/Σ(*w*(*F*_o²)²)]^{1/2}.

Table S2

Bond lengths:

Cd1—O9 ⁱ	2.131(8)	V2—O1 ^{iv}	1.947(10)
Cd1—O9	2.131(8)	V2—O5	1.972(11)
Cd1—O1W	2.21(2)	B1—O9	1.47(2)
Cd1—O1W ⁱ	2.21(2)	B1—O3	1.484(19)
Cd1—O6	2.463(10)	B1—O5	1.470(15)
Cd1—O6 ⁱ	2.463(10)	B1—O6 ⁱ	1.47(2)
V1—O2	1.567(12)	B2—O9	1.417(19)
V1—O1	1.890(9)	B2—O4 ^{iv}	1.458(18)
V1—O1 ⁱⁱ	1.940(9)	B2—O5 ^{iv}	1.502(18)
V1—O4	1.929(8)	B2—O8 ^v	1.480(17)
V1—O3	1.925(9)	B3—O8	1.312(14)
V2—O10	1.605(9)	B3—O6	1.319(17)
V2—O3 ⁱⁱⁱ	1.919(8)	B3—O7	1.356(14)
V2—O4 ^{iv}	1.927(8)		

Bond angles:

V(1)-O(1)-V(1) ^{vi}	147.8(5)	B(2) ⁱⁱⁱ -O(5)-B(1)	109.9(12)
V(1)-O(1)-V(2) ⁱⁱⁱ	101.3(4)	B(2) ⁱⁱⁱ -O(5)-V(2)	124.2(8)
B(1)-O(3)-V(2) ⁱⁱⁱⁱ	130.2(9)	B(1)-O(5)-V(2)	124.5(9)
B(1)-O(3)-V(1)	128.5(8)	B(3)-O(6)-B(1) ⁱ	120.7(11)
V(2) ⁱⁱⁱⁱ -O(3)-V(1)	101.3(4)	B(3)-O(6)-Cd(1)	143.0(8)
B(2) ⁱⁱⁱ -O(4)-V(1)	128.3(8)	B(1)-O(9)-B(2)	118.0(10)

B(2)ⁱⁱⁱ-O(4)-V(2)ⁱⁱⁱ 131.0(8) B(1)-O(9)-Cd(1) 105.4(8)

V(1)-O(4)-V(2)ⁱⁱⁱ 100.7(4) B(2)-O(9)-Cd(1) 131.5(8)

Symmetry operation: (i) 1.5-x, y, 0.5-z; (ii) 1+y, 0.5-z, 1.5-x; (iii) 1-y, -0.5+z, -0.5+x;
(iv) 0.5+z, 1-x, 0.5+y; (v) 1-z, -0.5+x, 0.5+y; (vi) 1.5-z, -1+x, 0.5-y.